Eur. Phys. J. C (2022) 82:637
https://doi.org/10.1140/epjc/s10052-022-10527-2

THE EUROPEAN PHYSICAL JOURNAL C

Regular Article - Theoretical Physics

Searching for a vector-like B quark through a tW decay channel at future electron–positron colliders

Lin Han[1,a], **Jie-Fen Shen**[1,b], **Yao-Bei Liu**[2]

[1] School of Biomedical Engineering, Xinxiang Medical University, Xinxiang 453003, People's Republic of China
[2] Henan Institute of Science and Technology, Xinxiang 453003, People's Republic of China

Received: 28 March 2022 / Accepted: 13 June 2022

Abstract Vector-like quarks are predicted by several theoretical scenarios of new physics which could solve the hierarchy problem in particular and might be produced through electroweak interactions. In this work, we investigate the prospects for discovering the $SU(2)$ singlet vector-like bottom quark (VLQ-B) in e^+e^- collisions at the future proposed 3 TeV Compact Linear Collider (CLIC). The analysis is performed within the framework of a simplified model featuring only two free parameters: the VLQ-B mass m_B and the coupling constant g^*. We study its single production process $e^+e^- \to B\bar{b}$ and perform a detailed analysis in the decay channel $B \to tW^-$ at the 3 TeV CLIC. The 2σ exclusion limit and 5σ discovery prospects are obtained for the model parameters, respectively. Our results show that the future CLIC will be an ideal hunting ground for such vector-like quarks which have electroweak interactions.

1 Introduction

Understanding the nature of the Higgs boson is one of the key elements for a full understanding of electroweak interactions and in particular of the breaking of electroweak symmetry. A very important question is the hierarchy problem of the weak scale [1]. Vector-like quarks (VLQs) are predicted to solve the gauge hierarchy problem in many new physics (NP) scenarios beyond the Standard Model (SM), such as little Higgs models [2], composite Higgs models [3–5], and other extended models [6–9]. Such new VLQs are color-triplet spin-1/2 fermions, and the left- and right-handed components transform with the same properties under the SM electroweak symmetry group [10]. Depending on the model, VLQs can be realized in different multiplets, such as electroweak singlet $[T, B]$, electroweak doublets $[(X, T), (T, B)$ or $(B, Y)]$, or electroweak triplets $[(X, T, B)$ or $(T, B, Y)]$ [11]. A common feature of these new fermions is that they can decay into a SM quark and a SM gauge boson, or a Higgs boson, which could generate characteristic signatures at the current and future high-energy colliders (for example, see [12–28]).

Up to now, the direct searches for VLQs have been performed by the ATLAS and CMS Collaborations in Run 2 [29–38]. Although there is no experimental evidence of such new particles, the constraints on their masses have been obtained at a 95% confidence level (CL). Given the current constraints from direct searches by the ATLAS [36] and CMS [37] Collaborations with an integrated luminosity of 35–36 fb^{-1}, the minimum mass of a VLQ is set at about 1.2–1.3 TeV for a variety of signatures via their pair production. Very recently, the CMS Collaboration presented a search for bottom-type vector-like (VLQ-B) pair production in the fully hadronic final state using Run 2 data with a total integrated luminosity of 137 fb^{-1} [38], and excluded their masses up to 1570, 1390, and 1450 GeV for 100% $B \to bh$, 100% $B \to tZ$, and BY doublet cases, respectively. Here, we focus on the SU(2) singlet VLQ-B with an electric charge of $-1/3e$, which couples exclusively to third-generation SM quarks, $B \to Wt, Hb, Zb$, since this is the scenario least constrained by previous measurements [13].

So far, most of the phenomenological analysis on the VLQ-B focuses on its single or pair production at the hadron colliders in a model-independent way [39–42]. Nevertheless, the LHC may not provide us with sufficient information about some couplings between the SM particles with the VLQs. Compared with hadron colliders, a future linear e^+e^- collider with energies on the teraelectron volt scale, extremely high luminosity, and very clean background environment can provide extended discovery potential for these new particles [43–45]; i.e., the final stage of the Compact Linear Collider (CLIC) operating at an energy of 3 TeV is expected to directly examine the pair production of a new heavy fermion of mass up to 1.5 TeV [46]. The future high-energy linear

[a] e-mail: hanlin@xxmu.edu.cn
[b] e-mail: shjf@xxmu.edu.cn (corresponding author)

Published online: 25 July 2022

e^+e^- collider is thus a precision machine with which the properties of new VLQs can be measured precisely once their masses are well known [47–52]. Related works regarding the single VLQ-B production at the future high-energy e^+e^- colliders were very recently carried out in Refs. [53–55] with decay channels $B \to tZ$ and $B \to th$. The benefit is that the single production processes have more potential than paired production due to lower phase space suppression. Because of the larger branching ratio $Br(B \to tW) \simeq 50\%$ for the heavy singlet VLQ-B, we focus herein on the observability of the singlet VLQ-B production at the future 3 TeV CLIC via the process $e^+e^- \to B(\to tW^-)\bar{b}$ combined with two types of final states. We expect that such work may become a complementary option to other decay channels in searches for the heavy VLQ-B at the future high-energy linear colliders.

This paper is organized as follows: In Sect. 2, we briefly review the couplings of VLQ-B with the SM particles and discuss its single production at the future 3 TeV CLIC via the $B \to tW$ decay channel. Section 3 is devoted to a detailed analysis of the signal and SM backgrounds. Finally, we summarize our results in Sect. 4.

2 Vector-like B quark in the simplified model

A prominent class of models predicting light spin-1/2 vector-like top and bottom partners is the class of composite Higgs models, such as the minimal composite Higgs scenario (with the coset structure SO(5)/SO(4); see e.g. [1]) and the TS-10 models (a four-dimensional version of a model with composite fermions in a 10 representation of SO(5); see e.g. [4,5]). It is clear that such VLQs share similar final-state topologies, with different branching ratios and single production couplings depending on the particular underlying model. Therefore, when looking for possible dedicated searches for such VLQs at the current and future high-energy colliders, it is preferable to use a simplified model approach, involving for example only the mass of the VLQ-B and its "single production" coupling as free parameters. Thus, we pursue this approach for the rest of the paper.

2.1 An effective Lagrangian for the singlet VLQ-B

Recently, a generic parametrization of an effective Lagrangian for such VLQs was proposed in [13], where the authors considered VLQs embedded in different representations of the weak SU(2) group, with other minimal assumptions regarding the structure of the couplings. In particular, VLQs which can mix and decay directly into all generations of SM quarks are included. Particularly interesting for our purposes is the case in which the VLQ-B is an SU(2) singlet, with couplings only to the third generation of SM quarks. The Lagrangian that parameterizes the VLQ-B couplings to quarks and electroweak boson can be expressed as [13]

$$\mathcal{L} = \frac{gg^*}{2}\left[\frac{1}{\sqrt{2}}\left[\bar{B}_L W^-_\mu \gamma^\mu t_L\right] + \frac{1}{2\cos\theta_W}\left[\bar{B}_L Z_\mu \gamma^\mu b_L\right] - \frac{m_B}{2m_W}\left[\bar{B}_R H b_L\right] - \frac{m_b}{2m_W}\left[\bar{B}_L H b_R\right]\right] + \text{h.c.}, \quad (1)$$

where g is the $SU(2)_L$ gauge coupling constant, θ_W is the Weinberg angle, and g^* stands for the coupling strength of the VLQ-B to SM quarks.[1]

Certainly, the mixing of the top and bottom quark with these new VLQs can offer new contributions to precisely measured observables of the SM, such as the oblique parameters S and T, and $Z \to b\bar{b}$ data; thus, the relevant model parameters can be constrained by the indirect searches of the electroweak precision observables (see [10] for a dedicated analysis of this model). However, such indirect bounds on the relevant mixing parameters are model-dependent and may be relaxed via cancellation of the contributions of different vector-like multiplets [56] (and/or other types of new physics models). Such models require dedicated examination of their electroweak constraints (see e.g. [57]) and are not covered by the analysis in this paper. For example, the existing limits on the couplings are estimated as $\kappa \leq 0.23$ for coupling to the third generation only [13]. Note also that the bounds may be weakened in specific models; therefore, here we consider only the direct bounds via the single production process of VLQs at the LHC. Recently, the authors of [22] studied the sensitivity in the plane of the coupling κ and VLQ mass M_Q using the CONTUR framework [58] and gave the disfavored regions at a 95% CL as $\kappa \in [0.1, 1]$ and $M_Q \in [1200\ \text{GeV}, 2000\ \text{GeV}]$. Thus, here we assume only a phenomenologically guided limit and take a conservative value $g^* \leq 0.5$ [29,30].

2.2 Single production of VLQ-B at the CLIC

In Fig. 1, we show the leading-order (LO) Feynman diagram of the process $e^+e^- \to B\bar{b}$ with the decay channel $B \to tW^-$.

In order to make a prediction for the signal, we calculate the LO cross section for the process $e^+e^- \to B\bar{b}$ ($b\bar{B}$) times the branching ratio of $B \to tW$ using MadGraph5-aMC@NLO [59] (henceforth MG5). Note that the model file of the singlet VLQ-B quark is publicly available online in the Feynrules repository [60]. In this case, the singlet VLQ-B has three different decay channels into SM particles: tW, bZ, and bH. Using the equivalence theorem [61–66], the branching fractions for these three decay modes are 0.5, 0.25, and 0.25,

[1] The coupling parameter can also be described as other constants, i.e., $\sin\theta$ [10] or κ [13]. After comparison, we find that there is a simple relation among these coupling parameters: $g^* = \sqrt{2}\sin\theta = \sqrt{2}\kappa$.

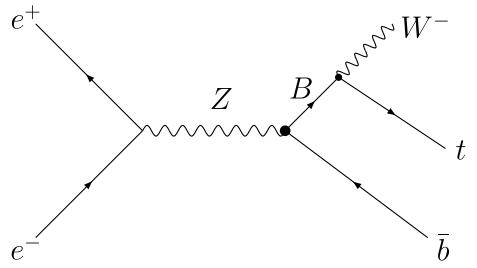

Fig. 1 Representative Feynman diagrams of the process $e^+e^- \to B(\to tW^-)\bar{b}$

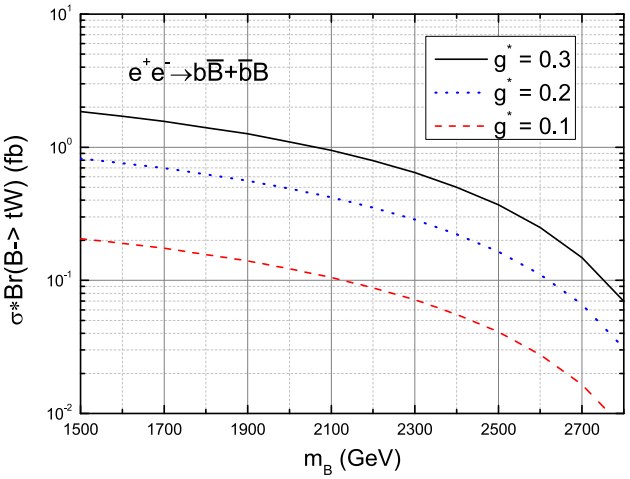

Fig. 2 Total cross sections as a function of m_B with three typical values of g^*

respectively. The numerical values of the input parameters are taken from [67].

In Fig. 2, we show the dependence of the cross section $\sigma(e^+e^- \to B\bar{b} + b\bar{B}) \times Br(B \to tW)$ on the B quark mass m_B at a 3 TeV CLIC for three typical values of g^*. As the VLQ-B quark mass grows, the cross section of single production decreases slowly due to a larger phase space. For $g^* = 0.2$ and $m_B = 1.5$ (2) TeV, the cross section can reach 0.82 (0.48) fb. Obviously, the cross section of single B-quark production is proportional to the square of the coupling strength g^* for a given B quark mass.

3 Collider simulation and analysis

Considering the subsequent decay mode of the gauge boson $W^\pm$, we focus on the 3 TeV CLIC and present our analysis for the $2\ell 2b + \not{E}_T$ final state, where $W^\pm$ is assumed to decay leptonically, and $\ell 2b2j + \not{E}_T$ final state where one $W^\pm$ decays leptonically and the other one decays hadronically.

In our simulation, we use MG5 to generate the parton-level events of signal and SM background, and these events are interfaced to Pythia 8.20 [68] for showering and hadronization. All event samples are fed into the Delphes 3.4.2 program [69] for detector simulation with the CLIC detector card designed for 3 TeV [70]. Jets are clustered according to the Valencia Linear Collider (VLC) algorithm [71,72] and fixed one-size parameter $R = 0.7$. The b-tagging efficiency is taken as the loose working points with 90% b-tagging efficiency in order not to excessively reduce the signal efficiency. The misidentification rates are given as a function of energy and pseudorapidity; i.e., in a bit where $E > 500$ GeV and $1.53 < |\eta| \leq 2.09$, misidentification rates are 5×10^{-2}. Finally, we use MadAnalysis5 [73] to analyze the signal and background events.

To identify objects, we first use the following basic cuts at the parton level for the signal and SM background:

$$p_T^\ell > 20\ \text{GeV}, \quad p_T^{j/b} > 25\ \text{GeV}, \quad |\eta_{\ell/b}| < 2.5, \quad |\eta_j| < 5, \tag{2}$$

where $p_T^{\ell,b,j}$, $|\eta_{\ell/b/j}|$ are the transverse momentum and pseudo-rapidity of leptons, b-jets, and light jets.

3.1 $2\ell 2b + \not{E}_T$ final state

We begin with the final state consisting of two same- or different- flavor and opposite-sign di-leptons along with two b-jets and missing energy $\not{E}_T$, which comes from the following process:

$$e^+e^- \to B(\to tW^-)\bar{b} \to t(\to b\ell^+\nu_\ell)W^-(\ell^-\bar{\nu}_\ell)\bar{b}. \tag{3}$$

The dominant background comes from the $2\ell 2b\not{E}_T$ final state comprising the following possible processes that lead to a similar final state:

- $e^+e^- \to tW^-\bar{b}(\bar{t}W^+b)$ with $t \to bW^+(\bar{t} \to \bar{b}W^-)$ and $W^+ \to \ell^+\nu_\ell$ ($W^- \to \ell^-\bar{\nu}_\ell$.
- $e^+e^- \to W^+W^-h$ with $W^+ \to \ell^+\nu_\ell$ ($W^- \to \ell^-\bar{\nu}_\ell$ and $h \to b\bar{b}$.
- $e^+e^- \to W^+W^-Z$ with $W^+ \to \ell^+\nu_\ell$ ($W^- \to \ell^-\bar{\nu}_\ell$ and $Z \to b\bar{b}$.
- $e^+e^- \to ZZZ$ with $Z \to \ell^+\ell^-$, $Z \to b\bar{b}$ and $Z \to \nu_\ell\bar{\nu}_\ell$.

According to the feature of the signal, the dominant SM backgrounds come from the single-top production processes, namely $e^+e^- \to tW^-\bar{b}, \bar{t}W^+b$, as shown in Fig. 3. Note that the contribution from the top pair production process $e^+e^- \to t\bar{t}$ is also included with the $t \to Wb$ decay. For the center-of-mass energy $\sqrt{s} = 3$ TeV, the relatively large contribution for the tWb final state comes from the t-channel single-top production process [74]. Here, we do not consider the $e^+e^- \to W^+W^-Z$, $e^+e^- \to W^+W^-h$, and $e^+e^- \to ZZZ$ production processes because their cross sections are negligible after applying our selection cuts (see below).

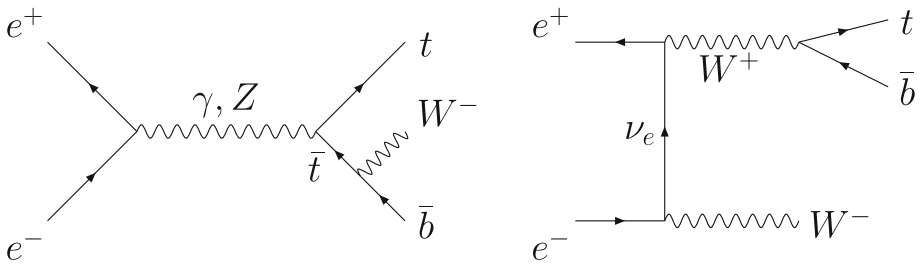

Fig. 3 Representative Feynman diagrams of the single-top production process $e^+e^- \to tW^-\bar{b}$

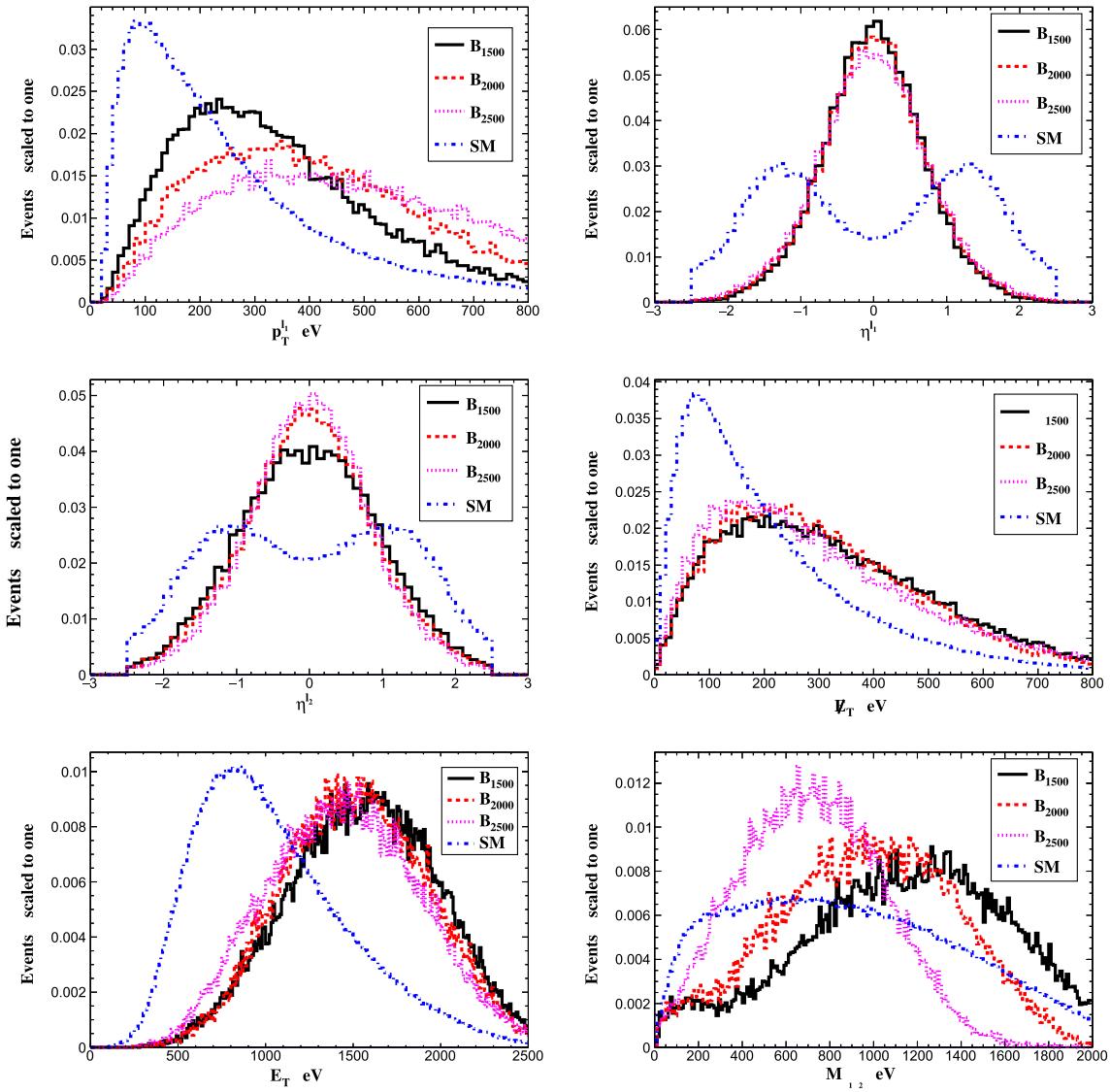

Fig. 4 Normalized distributions for the signals (with $m_B = 1500$, 2000, and 2500 GeV) and SM background at the CLIC

In Fig. 4, we draw some differential normalized distributions for signals and SM backgrounds, including the transverse momentum distributions of lepton (p_T^ℓ), the normalized pseudo-rapidity distribution of the lepton, the scalar sum of the transverse energy of all final-state objects E_T, and the missing energy $\not{E}_T$. For the background, the leptons can be produced via the s-channel exchange of γ and Z, as well as t-channel exchange of neutrinos, which results in the peaks at higher η values. However, for the signal, the leptons are produced from the decay of the $W^\pm$, which are generated from the decay of the heavier VLQ-B, produced via the s-channel exchange of Z. As a result, the η distribution for the signal is more centrally peaked. We carry out the cut-based analysis by looking at some relevant kinematic variables which

Table 1 Cut flow of the cross sections (in fb) for the signals and SM background at the 3 TeV CLIC with $g^* = 0.3$ and two typical VLQ-B quark masses

Cuts	Signals		Background
	1500 GeV	2000 GeV	
Basic	0.015	0.009	0.3
Cut 1	0.011	0.006	0.13
Cut 2	0.006	0.004	0.032
Cut3	0.004	0.0027	0.015

Table 2 Cut flow of the cross sections (in fb) for the signals and SM background at the 3 TeV CLIC with $g^* = 0.3$ for the $\ell 2b2j + \not{E}_T$ final state

Cuts	Signals		Background
	1500 GeV	2000 GeV	
Basic	0.055	0.032	0.43
Cut 1	0.042	0.027	0.19
Cut 2	0.029	0.021	0.032
Cut 3	0.021	0.016	0.02

can help design proper cuts (Cut 1, Cut 2, Cut 3) on them to improve the signal over the background.

- Cut 1: The transverse missing energy is required $\not{E}_T > 200$ GeV.
- Cut 2: There are exactly two isolated leptons ($N(\ell) = 2$) with $|\eta_{\ell_1}| \leq 1$ and $|\eta_{\ell_2}| \leq 1$. Besides, the transverse momentum of the leading lepton is required to have $p_T^{\ell_1} > 200$ GeV.
- Cut 3: The scalar sum of the transverse energy of all final-state objects E_T is required to be $E_T > 1100$ GeV. At the same time, we also demand $M_{b_1 b_2} > 200$ GeV to reduce the backgrounds coming from $Z \to b\bar{b}$ and $h \to b\bar{b}$.

We present the cross sections for the signals ($m_B = 1500, 2000$ GeV) and the SM background after imposing the cuts in Table 1. One can see that the SM background is suppressed very efficiently, while the signals still have relatively good efficiency at the end of the cut flow.

3.2 $\ell 2b2j + \not{E}_T$ final state

Considering the subsequent decay channel $W^- \to \ell^- \bar{\nu}_\ell$ and $t \to bW^+ \to bjj$, we consider the following process as the signal:

$$e^+e^- \to B(\to tW^-)\bar{b} \to t(\to bjj)W^-(\ell^-\bar{\nu}_\ell)\bar{b}. \quad (4)$$

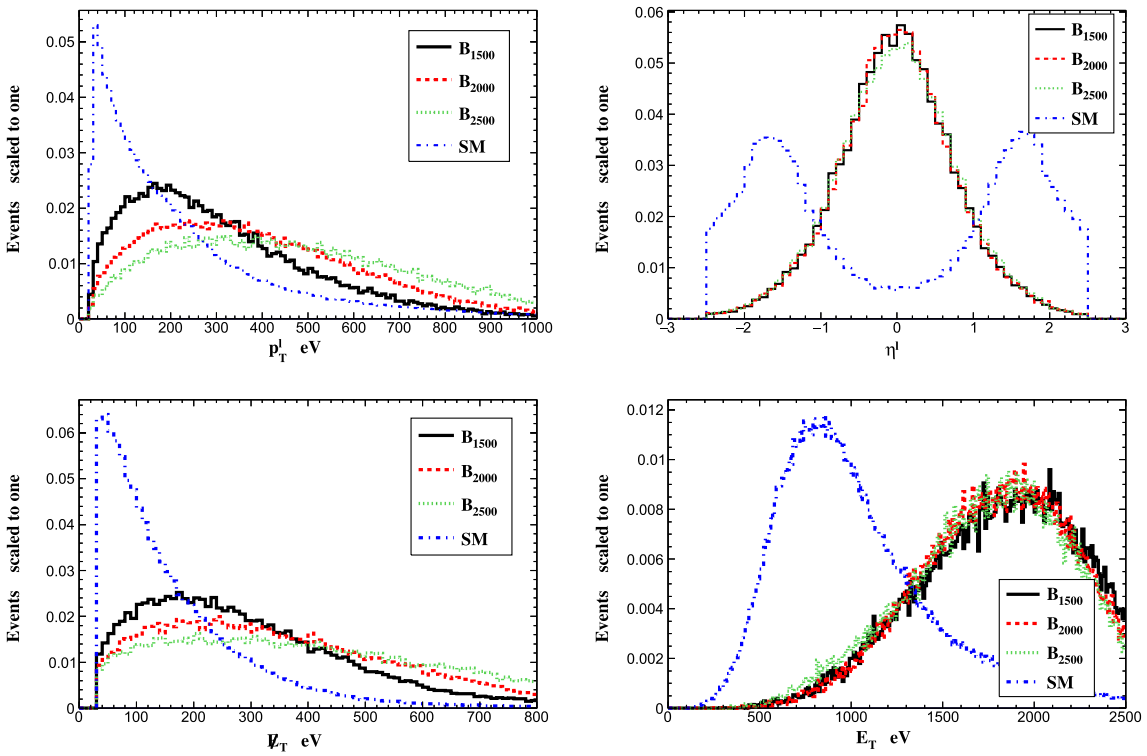

Fig. 5 Same as Fig. 4 but for the $\ell 2bjj + \not{E}_T$ final state

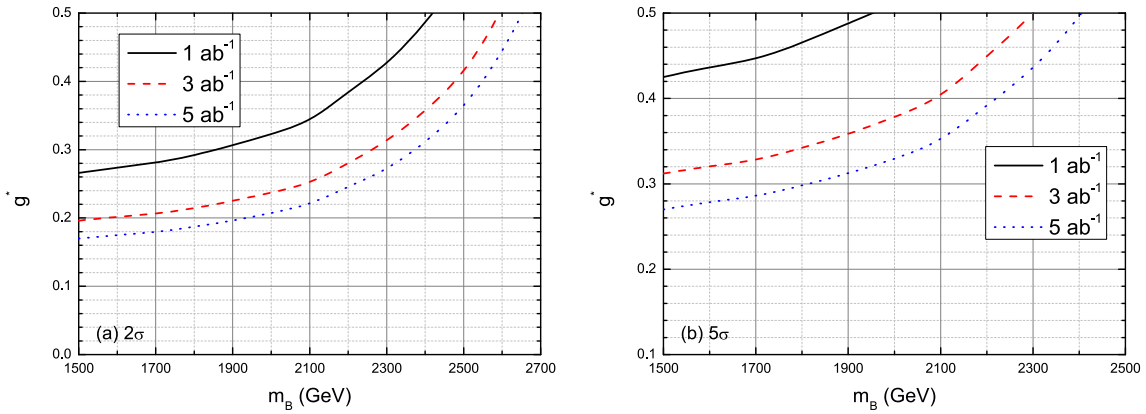

Fig. 6 2σ exclusion limit (left) and 5σ discovery prospects (right) contour plots for the $2\ell 2b + \not{E}_T$ final state in $g^* - m_B$ planes at the 3 TeV CLIC with three typical integral luminosity values

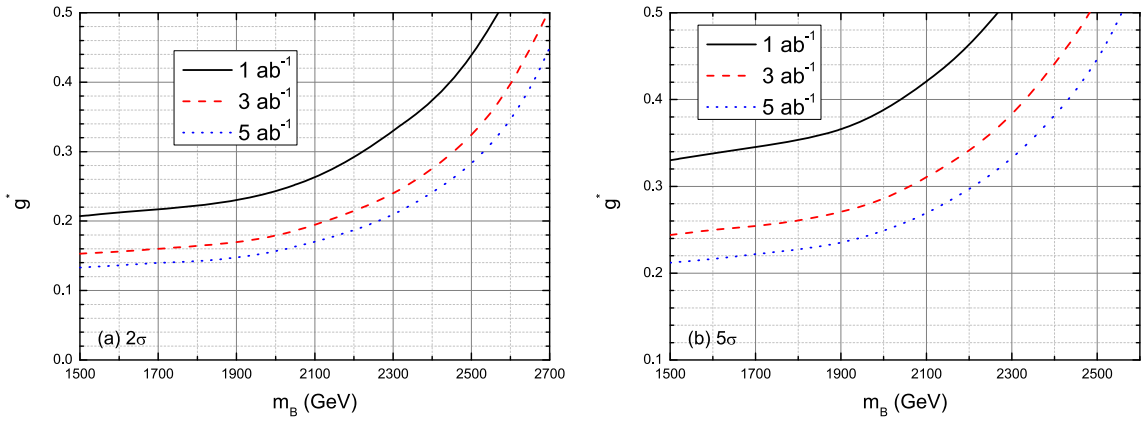

Fig. 7 Same as Fig. 6 but for the $\ell 2bjj + \not{E}_T$ final state

Similarly, according to the differential distributions in Fig. 5, we implement the following cuts to suppress the background:

- Cut 1: It is required that the transverse missing energy $\not{E}_T > 150$ GeV.
- Cut 2: There are exactly one isolated leptons ($N(\ell) = 1$) with $p_T^\ell > 150$ GeV and $|\eta_\ell| \leq 1$.
- Cut 3: The scalar sum of the transverse energy of all final-state objects E_T is required to be $E_T > 1300$ GeV. We also demand $M_{b_1 b_2} > 150$ GeV to exclude the WWZ and WWh backgrounds.

From Table 2, we found substantial suppression on the SM background once the kinematical cuts were imposed.

3.3 Discovery and exclusion significance

Then, we estimate the expected discovery and exclusion significance by using the median significance $\mathcal{Z}$ [75]:

$$\mathcal{Z}_{\rm disc} = \sqrt{2[(s+b)\ln(1+s/b) - s]} \geq 5,$$

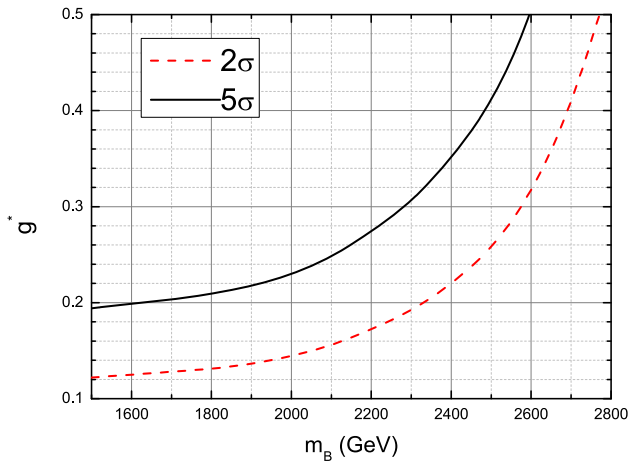

Fig. 8 Combined 2σ exclusion limit and 5σ discovery prospect contour plots for the signal in $g^* - m_B$ planes at the CLIC with an integral luminosity of 5 ab^{-1}

$$\mathcal{Z}_{\rm excl} = \sqrt{2[s - b\ln(1+s/b)]} \leq 2 \qquad (5)$$

where s and b are the signal and background events, respectively. Note that here we do not consider the effects of the

Table 3 Some results of searching for VLQ-B at different colliders

Channel	Data set	Excluding capability		Discovery capability		Reference
		g^* (κ_B)	m_B/GeV	g^* (κ_B)	m_B/GeV	
$B \to bZ$	HL-LHC@3 ab^{-1}	[0.14, 0.5]	[1300, 2000]	[0.24, 0.5]	[1300, 1700]	[26]
$B \to bh$	CLIC@5 ab^{-1}	[0.09, 0.15]	[1300, 2000]	[0.14, 0.24]	[1300, 2000]	[53]
$B \to bZ$	CLIC@5 ab^{-1}	[0.16, 0.5]	[1200, 2400]	[0.26, 0.5]	[1200, 2150]	[54]
$B \to tW$	CLIC@5 ab^{-1}	[0.12, 0.4]	[1500, 2700]	[0.2, 0.5]	[1500, 2600]	This work

systematic uncertainties, the initial state radiation, or beamstrahlung, but we expect these will not change our results significantly.

In Figs. 6 and 7, we plot the 2σ and 5σ sensitivity reaches for the coupling strength g^* as a function of m_B at the 3 TeV CLIC with three typical integral luminosity values: 1, 3, and 5 ab^{-1}. One finds that for the $2\ell 2b + \not{E}_T$ final state, the VLQ-B quark can be excluded in the region of $g^* \in [0.2, 0.5]$ $[0.17, 0.44]$ and $m_B \in$ [1500 GeV, 2600 GeV] at the 3 TeV CLIC with integrated luminosity of 3 (5) ab^{-1}, while the discover region can reach $g^* \in [0.31, 0.5]$ $[0.27, 0.43]$ and $m_B \in$ [1500 GeV, 2300 GeV]. Similarly, for the $\ell 2bjj + \not{E}_T$ final state, the VLQ-B quark mass can be excluded in the region of $g^* \in [0.15, 0.5]$ $[0.13, 0.44]$ and $m_B \in$ [1500 GeV, 2700 GeV], and the discover region can reach $g^* \in$ $[0.24, 0.5]$ $[0.21, 0.44]$ and $m_B \in$ [1500 GeV, 2500 GeV].

Then, we combine its sensitivity with the above two types of final states by using $\mathcal{Z}_{\rm comb} = \sqrt{\mathcal{Z}_1^2 + \mathcal{Z}_2^2}$. For comparison, we further present in Fig. 8 the combined sensitivity reaches for the coupling strength g^* as a function of the VLQ-B quark mass m_B. One can see that the B quark can be excluded in the region of $g^* \in [0.12, 0.4]$ and $m_B \in$ [1500 GeV, 2700 GeV] at the 3 TeV CLIC with the integrated luminosity of 5 ab^{-1}, while the discover region can reach $g^* \in [0.2, 0.5]$ and $m_B \in$ [1500 GeV, 2600 GeV]. Moreover, we list some existing results related to searching for the VLQ-B in Table 3. We can find that our result is competitive and complementary compared with the other sensitive channels in previous studies.

4 Conclusion

Vector-like quarks that couple preferentially to third-generation Standard Model (SM) quarks are a well-motivated extension of the SM, which could specifically solve the hierarchy problem. In this study we have searched for accessible limits for the SU(2) singlet VLQ-B at the future 3 TeV CLIC via the process $e^+e^- \to B\bar{b} \to tW^-\bar{b}$ through the $B \to tW^-$ channel in a simplified model. We performed a full simulation for the signals and the relevant SM backgrounds with the CLIC detector card designed for 3 TeV. Our numerical results show that, at the 3 TeV CLIC with an integrated luminosity of 5 ab^{-1}, the VLQ-B can be excluded in the region of $g^* \in [0.12, 0.4]$ and $m_B \in$ [1500 GeV, 2700 GeV] and the discover region can reach $g^* \in [0.2, 0.5]$ and $m_B \in$ [1500 GeV, 2600 GeV]. Thus, the future 3 TeV CLIC will prove to be an ideal hunting ground for such vector-like quarks which have electroweak strength interactions.

Acknowledgements The work is supported by the Foundation of the Key Research Projects in Universities of Henan (22A140019) and the Natural Science Foundation of Henan Province (222300420443).

Data Availability Statement This manuscript has no associated data or the data will not be deposited. [Authors' comment: All data has been included in the table and figures.]

Funded by SCOAP^3. SCOAP^3 supports the goals of the International Year of Basic Sciences for Sustainable Development.

References

1. A. De Simone, O. Matsedonskyi, R. Rattazzi and A. Wulzer, JHEP 04, 004 (2013)
2. N. Arkani-Hamed, A. G. Cohen, E. Katz and A. E. Nelson, JHEP 0207, 034 (2002)
3. K. Agashe, R. Contino, and A. Pomarol, Nucl. Phys. B 719 (2005) 165
4. N. Vignaroli, JHEP 07, 158 (2012)
5. N. Vignaroli, Phys. Rev. D **86**, 115011 (2012)
6. H.J. He, T.M.P. Tait, C.P. Yuan, Phys. Rev. D **62**, 011702 (2000)
7. X. F. Wang, C. Du and H. J. He, Phys. Lett. B 723, 314–323 (2013)
8. H.J. He, C.T. Hill, T.M.P. Tait, Phys. Rev. D **65**, 055006 (2002)
9. H. J. He and Z. Z. Xianyu, JCAP 10, 019 (2014)
10. J.A. Aguilar-Saavedra, R. Benbrik, S. Heinemeyer, M. Pérez-Victoria, Phys. Rev. D **88**, 094010 (2013)

11. F. del Aguila, M. Perez-Victoria and J. Santiago, JHEP 09, 11 (2000)
12. A. Atre, G. Azuelos, M. Carena, T. Han, E. Ozcan, J. Santiago and G. Unel, JHEP 1108, 080 (2011)
13. M. Buchkremer, G. Cacciapaglia, A. Deandrea and L. Panizzi, Nucl. Phys. B 876, 376 (2013)
14. D. Barducci and L. Panizzi, JHEP 12, 057 (2017)
15. G. Cacciapaglia, A. Carvalho, A. Deandrea, T. Flacke, B. Fuks, D. Majumder, L. Panizzi and H. S. Shao, Phys. Lett. B 793, 206–211 (2019)
16. S. Yang, J. Jiang, Q. S. Yan and X. Zhao, JHEP 09, 035 (2014)
17. Y. B. Liu, Nucl. Phys. B 923, 312–323 (2017)
18. Y. B. Liu and Y. Q. Li, Eur. Phys. J. C 77, no.10, 654 (2017)
19. Y.B. Liu, S. Moretti, Phys. Rev. D **100**(1), 015025 (2019)
20. X.Y. Tian, L.F. Du, Y.B. Liu, Nucl. Phys. B **965**, 115358 (2021)
21. S. Moretti, D. O'Brien, L. Panizzi, H. Prager, Phys. Rev. D **96**(7), 075035 (2017)
22. A. Buckley, J. M. Butterworth, L. Corpe, D. Huang and P. Sun, SciPost Phys. 9, no.5, 069 (2020)
23. A. Deandrea, T. Flacke, B. Fuks, L. Panizzi and H. S. Shao, JHEP 08, 107 (2021)
24. S. J. D. King, S. F. King, S. Moretti and S. J. Rowley, JHEP 21, 144 (2020)
25. K. Cheung, W. Y. Keung, C. T. Lu and P. Y. Tseng, JHEP 05, 117 (2020)
26. J.Z. Han, J. Yang, S. Xu, H.K. Wang, Nucl. Phys. B **975**, 115672 (2022)
27. X. Qin, L.F. Du, J.F. Shen, Nucl. Phys. B **979**, 115784 (2022)
28. S. Balaji, JHEP 05, 015 (2022)
29. M. Aaboud et al. (ATLAS), JHEP **05**, 164 (2019)
30. A.M. Sirunyan et al. (CMS), Eur. Phys. J. C **79**, 90 (2019)
31. M. Aaboud et al. (ATLAS), Phys. Rev. D **98**(9), 092005 (2018)
32. M. Aaboud et al. (ATLAS), JHEP **1812**, 039 (2018)
33. M. Aaboud et al. (ATLAS), JHEP **1808**, 048 (2018)
34. A.M. Sirunyan et al. (CMS), Eur. Phys. J. C **79**(4), 364 (2019)
35. A.M. Sirunyan et al. (CMS), Phys. Rev. D **100**, 072001 (2019)
36. M. Aaboud et al. (ATLAS), Phys. Rev. Lett. **121**, 211801 (2018)
37. A.M. Sirunyan et al. (CMS), JHEP **08**, 177 (2018)
38. A.M. Sirunyan et al. (CMS), Phys. Rev. D **102**, 112004 (2020)
39. J. Nutter, R. Schwienhorst, D.G.E. Walker, J.H. Yu, Phys. Rev. D **86**, 094006 (2012)
40. X. Gong, C. X. Yue and Y. C. Guo, Phys. Lett. B 793, 175–180 (2019)
41. X. Gong, C. X. Yue, H. M. Yu and D. Li, Eur. Phys. J. C 80, no.9, 876 (2020)
42. D. Choudhury, K. Deka, N. Kumar, Phys. Rev. D **104**(3), 035004 (2021)
43. H. Abramowicz et al. (CLIC Detector and Physics Study), arXiv:1307.5288 [hep-ex]
44. J. de Blas, R. Franceschini, F. Riva, P. Roloff, U. Schnoor, M. Spannowsky, J.D. Wells, A. Wulzer, J. Zupan, S. Alipour-Fard et al., arXiv:1812.02093 [hep-ph]
45. R. Franceschini, Int. J. Mod. Phys. A 35, 2041015 (2020)
46. D. Dannheim, P. Lebrun, L. Linssen, D. Schulte, S. Stapnes, arXiv:1305.5766 [physics.acc-ph]
47. R. Kitano, T. Moroi, S.F. Su, JHEP 12, 011 (2002)
48. K. Kong and S. C. Park, JHEP 08, 038 (2007)
49. A. Senol, A. T. Tasci and F. Ustabas, Nucl. Phys. B 851, 289–297 (2011)
50. K. Harigaya, S. Matsumoto, M.M. Nojiri, K. Tobioka, JHEP **01**, 135 (2012)
51. L. Guo, W. Liu, W. G. Ma, R. Y. Zhang, W. J. Zhang, A.B. Mahfoudh, Commun. Theor. Phys. 62(6), 824–832 (2014)
52. Y. B. Liu and Z. J. Xiao, Nucl. Phys. B 892, 63–82 (2015)
53. X. Qin, J.F. Shen, Nucl. Phys. B **966**, 115388 (2021)
54. L. Han and J. F. Shen, Eur. Phys. J. C 81, no.5, 463 (2021)
55. J.Z. Han, J. Yang, S. Xu, H.K. Wang, Phys. Rev. D **105**(1), 015005 (2022)
56. K. Agashe, R. Contino, L. Da Rold and A. Pomarol, Phys. Lett. B 641, 62–66 (2006)
57. C. Anastasiou, E. Furlan, J. Santiago, Phys. Rev. D **79**, 075003 (2009)
58. J. M. Butterworth, D. Grellscheid, M. Krämer, B. Sarrazin and D. Yallup, JHEP 03, 078 (2017)
59. J. Alwall, R. Frederix, S. Frixione, V. Hirschi, F. Maltoni, O. Mattelaer, H.-S. Shao, T. Stelzer, P. Torrielli and M. Zaro, JHEP 1407 (2014) 079
60. http://feynrules.irmp.ucl.ac.be/wiki/VLQ-bsingletvl. Accessed May 2017
61. H.J. He, Y.P. Kuang, C.P. Yuan, For a comprehensive review. arXiv:hep-ph/9704276
62. H.J. He, Y.P. Kuang, X.Y. Li, Phys. Rev. Lett. **69**, 2619–2622 (1992)
63. H.J. He, Y.P. Kuang, X.Y. Li, Phys. Rev. D 49, 4842–4872 (1994)
64. H. J. He, Y. P. Kuang and C. P. Yuan, Phys. Rev. D 51, 6463–6473 (1995)
65. H. J. He, Y. P. Kuang and C. P. Yuan, Phys. Rev. D 55, 3038–3067 (1997)
66. H. J. He and W. B. Kilgore, Phys. Rev. D 55, 1515–1532 (1997)
67. M. Tanabashi et al. (Particle Data Group), Phys. Rev. D **98**, 030001 (2018)
68. T. Sjöstrand, S. Ask and J. R. Christiansen et al., Comput. Phys. Commun. 191, 159 (2015)
69. J. de Favereau et al. (DELPHES 3), JHEP **02**, 057 (2014)
70. E. Leogrande, P. Roloff, U. Schnoor, M. Weber, arXiv:1909.12728 [hep-ex]
71. M. Boronat, J. Fuster, I. Garcia, E. Ros and M. Vos, Phys. Lett. B 750, 95–99 (2015)
72. M. Boronat, J. Fuster, I. Garcia, P. Roloff, R. Simoniello and M. Vos, Eur. Phys. J. C 78, no.2, 144 (2018)
73. E. Conte, B. Fuks and G. Serret, Comput. Phys. Commun. 184, 222–256 (2013)
74. J. Fuster, I. García, P. Gomis, M. Perelló, E. Ros and M. Vos, Eur. Phys. J. C 75, 223 (2015)
75. G. Cowan, K. Cranmer, E. Gross, O. Vitells, Eur. Phys. J. C **71**, 1554 (2011). [Erratum: Eur. Phys. J. C **73**, 2501 (2013)]